J Appl Electrochem (2010) 40:1575–1582
DOI 10.1007/s10800-010-0164-0

REVIEW ARTICLE

Effect of some tripodal bipyrazolic compounds on C38 steel corrosion in hydrochloric acid solution

B. Zerga · A. Attayibat · M. Sfaira · M. Taleb · B. Hammouti · M. Ebn Touhami · S. Radi · Z. Rais

Received: 20 October 2009 / Accepted: 12 June 2010 / Published online: 15 July 2010

Abstract The corrosion inhibition of C38 steel in molar HCl by *N*,*N*-bis[2-(3,5-dimethyl-1H-pyrazol-1-yl)ethyl]buthylamine (P1) and 5-{*N*,*N*-bis[2-(3,5-dimethyl-1H-pyrazol-1-yl)ethyl] amino} pentanol (P2) has been investigated at 308 K using electrochemical and weight loss measurements. Measurements show that these compounds act as good inhibitors without changing the mechanism of the corrosion process. Moreover, the inhibiting efficiency increases with the increase in concentration of the studied inhibitors. Compound P2 showed better protection properties even at relatively higher temperatures when compared to P1. The associated activation corrosion and free adsorption energies have been determined. P1 and P2 are adsorbed on the C38 steel surface according to a Langmuir isotherm adsorption model.

Keywords C38 steel · Bipyrazolic tripod · Hydrochloric acid · Adsorption · 1 M HCl

B. Zerga · M. Sfaira (✉) · M. Taleb · Z. Rais
Laboratoire d'Analyses Physico-chimiques et Matériaux Catalytiques pour l'Environnement, Faculté des Sciences Dhar El Mahraz, BP 1796, 30000 Atlas, Fès, Morocco
e-mail: msfaira@yahoo.fr

A. Attayibat · S. Radi
LCOMPN-URAC25, Faculté des Sciences, Université Mohammed Premier, BP 717, 60000 Oujda, Morocco

B. Hammouti (✉)
LCAE-URAC18, Faculté des Sciences, Université Mohammed Premier, BP 717, 60000 Oujda, Morocco
e-mail: hammoutib@yahoo.fr

M. Ebn Touhami
Laboratoire d'Electrochimie, Corrosion et Environnement, Faculté des Sciences, BP 133, 14000 Kénitra, Morocco

1 Introduction

The C38 steel corrosion in acid media and especially in hydrochloric acid is often a very worrying problem for some industrial facilities; several researchers devoted their attention to develop more effective and non-toxic inhibitors to reduce both acid attack and protection aspects [1–6].

The use of organic compounds based corrosion inhibitors against metal dissolution is often associated with chemical and/or physical adsorption, involving a variation in the charge of adsorbed substance and a transfer of charge from one phase to the other. Special attention was paid to the effect of electron donating on the atom, electron withdrawing or groups responsible for adsorption and hence on the inhibitor performance. Furthermore, it has been observed that the adsorption mainly depends on steric factors, aromaticity, the structural properties of the organic compounds studied such as the presence of π-electrons and heteroatoms, which induce greater adsorption of the inhibitor molecules onto the surface of C38 steel [7–9]. The effect of temperature on the corrosion behaviour was also studied in the range of temperature from 313 to 353 K. Kinetic and activation parameters that govern metal corrosion have been evaluated and discussed.

The aim of this paper is to evaluate the corrosion inhibition efficiency and analyse the inhibitive mechanism of C38 steel corrosion in hydrochloric acid by: *N*,*N*-bis[2-(3,5-dimethyl-1H-pyrazol-1-yl)ethyl]buthylamine (P1) and 5-{*N*,*N*-bis[2-(3,5-dimethyl-1H-pyrazol-1-yl)ethyl] amino}pentanol (P2). Figure 1 shows the molecular structure of the investigated organic compounds P1 and P2, which were prepared according to previously reported an experimental procedure [10]. The inhibiting efficiency calculation is conducted using several weight loss and electrochemical techniques include dc

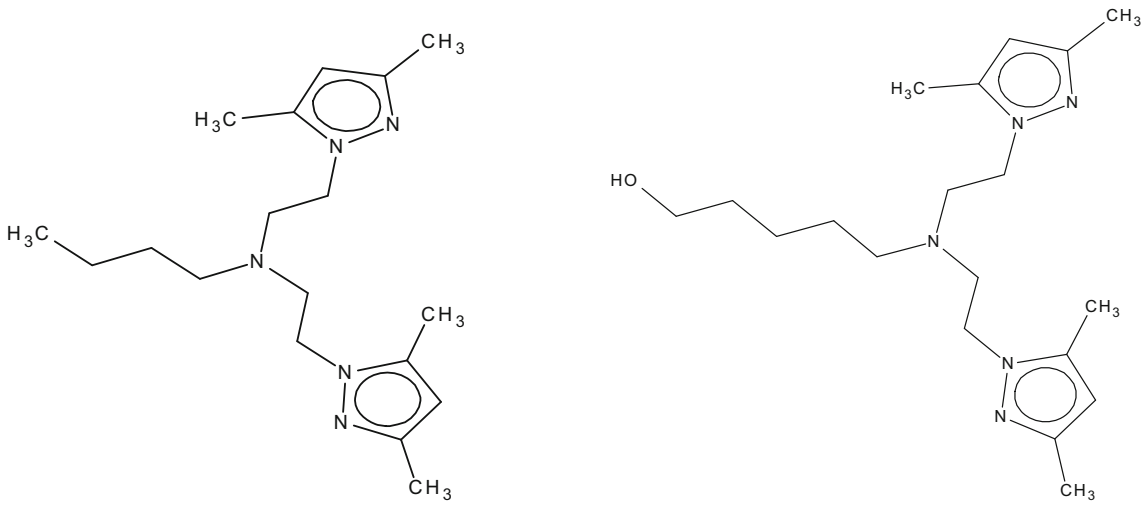

Fig. 1 Molecular structure of the studied bipyrazolic compounds

current–voltage and ac electrochemical impedance spectroscopy (EIS).

2 Experimental procedure

2.1 Material preparation

C38 steel strips containing (in wt%) 0.09 P, 0.38 Si, 0.01 Al, 0.05 Mn, 0.21 C, 0.05 S and balance iron were used for electrochemical and gravimetric studies. C38 steel specimens were mechanically polished on wet SiC papers (400, 600, 1000, and 1200), washed with double-distilled water, degreased ultrasonically in ethanol, and finally dried at room temperature before being immersed in the acid solution. The aggressive solution (1 M HCl), used as blank, was prepared by dilution of analytical grade 37%. Appropriate concentrations of inhibitors were prepared with double-distilled water addition. The concentration range of inhibitors employed was 10^{-6}–10^{-3} M in 1 M HCl. The temperature was controlled at 308 K without bubbling in a double walled glass cell.

2.2 Electrochemical measurements

Electrochemical measurements were carried out in a conventional three-electrode glass cell with a platinum counter electrode and a saturated calomel electrode (SCE) as reference. All tests were performed in continuously stirred conditions at room temperature; all tests were performed at 308 K. Potentiodynamic curves-polarization experiments were carried by (Radiometer-analytical PGZ 100) and controlled with analysis software (Voltamaster 4). The C38 steel electrode was maintained at open circuit conditions (corrosion potential, E_{corr}) for 1 h and thereafter prepolarized at −800 mV for 10 min. After this scan, the potential was swept to anodic potentials. The anodic and cathodic polarization curves were recorded at scan rate of 1 mV s^{-1}.

The EIS measurements were performed using a transfer function analyser (Voltalab PGZ 100), with a small amplitude a.c. signal (10 mV rms) over a frequency domain from 100 kHz to 10 MHz at 308 K with five points per decade. Computer programs automatically controlled the measurements performed at rest potentials after 1 h of immersion at E_{corr}. The impedance diagrams were given in the Nyquist representation.

In order to ensure reproducibility, all experiments were repeated three times. The evaluated accuracy was within 10%.

2.3 Weight loss measurements

Gravimetric experiments were investigated in a double-walled glass cell equipped with a thermostat cooling condenser. The solution volume was 100 cm^3 and the temperature of 308 K was controlled thermostatically. The C38 steel specimens were rectangular in the form (1 cm × 4 cm × 0.06 cm). The weight loss of C38 steel in 1 mol L^{-1} HCl with and without addition of inhibitors was determined after an immersion period in acid for 24 h. After the corrosion test, the specimens were carefully washed in double distilled water, dried and then weighted. Triplicate experiments were performed in each case, and the mean value of the weight loss is reported. Weight loss allowed us to calculate the mean corrosion rate as expressed in mg cm^{-2} h^{-1}.

3 Results and discussion

3.1 Polarization measurements

Polarisation curves, obtained in the presence and absence of P1 and P2, after prepolarizing the electrode at its E_{corr} for 1 h, are shown in Figs. 2 and 3, respectively. The potential was swept stepwise from the most cathodic potential to the anodic direction.

From these results, it appears that the increase in P1 and P2 concentration have no definite trend in the shift of corrosion potential values. As it can be seen, both cathodic and anodic reactions of C38 steel electrode corrosion were inhibited with the increase of P1 and P2 concentration in 1 mol L^{-1} HCl. Beside, P1 and P2 slow down the cathodic reaction to greater extents than the anodic one, especially at lower concentrations. This result suggests that the addition of P1 and P2 reduces anodic dissolution and lowers the reaction of hydrogen discharge. Moreover, Figs. 2 and 3 indicate that cathodic current–potential curves give rise to Tafel lines, indicating that the hydrogen evolution reaction is activation-controlled. Similar results were obtained with other series of bipyrazolic derivatives [11]. In contrast, the anodic curves show that the inhibition mode depends upon electrode potential. Indeed for an over voltage more than −0.25 V_{SCE}, the presence of P1 and P2 does not modify the I–E characteristics which indicates that significant dissolution process dominates the inhibition one. Therefore, in the vicinity of E_{corr}, an appreciable decrease in the current density is observed beyond 10^{-4} and 10^{-3} mol L^{-1} for P1 and P2, respectively. This phenomenon reflects the formation of anodic protective film on the electrode surface. Based on the marked decrease of the cathodic current densities and at potentials more negative than −0.25 V_{SCE}, in the anodic range, upon introducing the inhibitors in the aggressive solution, the inhibitors are considered as mixed type inhibitors with cathodic predominance. Analogue

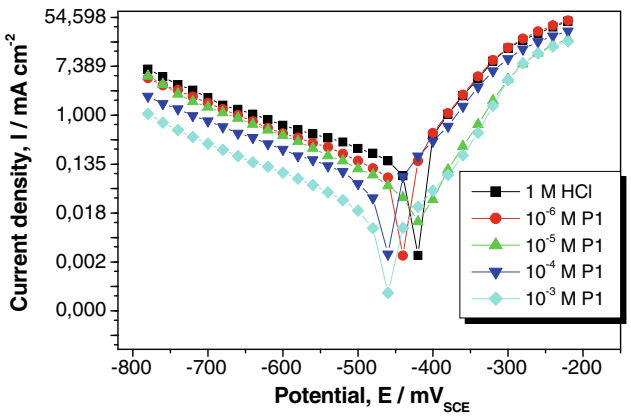

Fig. 2 Polarization curves for C38 steel in 1 mol L^{-1} HCl at different concentrations of P1

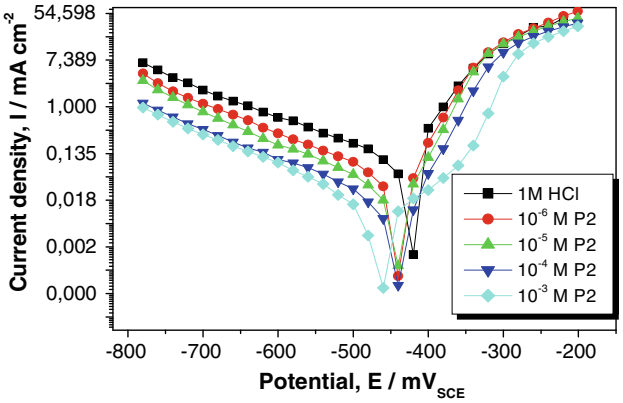

Fig. 3 Polarization curves for C38 steel in 1 mol L^{-1} HCl at different concentrations of P2

behaviour was observed in our earlier results [7, 12] and with other co-workers [13, 14].

The electrochemical parameters such as corrosion potential (E_{corr}), corrosion current density (I_{corr}), cathodic Tafel slope (βc) derived from polarization curves, and corresponding inhibition efficiency $E_I(\%)$ values at different inhibitors concentrations are given in Table 1. The inhibiting efficiency was derived from the Eq. 1:

$$E_I\% = \frac{I_{corr} - I'_{corr}}{I_{corr}} \times 100 \quad (1)$$

where, I_{corr} and I'_{corr} are the corrosion current densities values without and with inhibitors, respectively and determined by extrapolation of cathodic Tafel lines to the respective corrosion potentials.

From Table 1, it can be concluded that with the increase in concentration of both the additives P1 and P2, I_{corr} values decreases gradually at all the studied concentrations. Beside the inhibition efficiency $E_I\%$ increases with inhibitors concentration, reaching the values of 91 and 95% at 10^{-3} mol L^{-1} of P1 and P2, respectively. Based on all studied concentration of P1 and P2, these last can be ranked as follows: P2 > P1. The almost non-change of cathodic slope ($|\beta_c|$ remains ca. constant) indicates that the mechanism of hydrogen reaction reduction is not affected upon the addition of P1 and P2 concentration.

3.2 EIS measurements

Impedance measurements of the steel electrode at its open circuit potential after 1 h of immersion in 1 mol L^{-1} HCl solution alone and in the presence of various concentration of the best inhibitor P2. The recorded EIS spectra in uninhibited and inhibited medium show one depressive capacitive loop. The depressed semicircular appearance is often attributed to Cole–Cole [15, 16] and/or Cole–Davidson [17] representations and referred to frequency

Table 1 Polarization parameters and corresponding inhibition efficiency for the corrosion of the steel in 1 mol L^{-1} HCl without and with addition of various concentrations of bipyrazolic compounds P1 and P2

Inhibitors	Concentration (mol L^{-1})	E_{corr} (mV_{SCE})	$-\beta_c$ (mV $decade^{-1}$)	I_{corr} (μA cm^{-2})	E_I (%)
1 mol L^{-1} HCl	0	−419	168.7	144	–
P1	10^{-6}	−440	169.4	81	44
	10^{-5}	−419	166.0	51	65
	10^{-4}	−461	167.7	41	71
	10^{-3}	−460	164.8	14	91
P2	10^{-6}	−439	165.4	90	38
	10^{-5}	−440	170.0	36	75
	10^{-4}	−439	166.1	18	88
	10^{-3}	−459	169.3	8	95

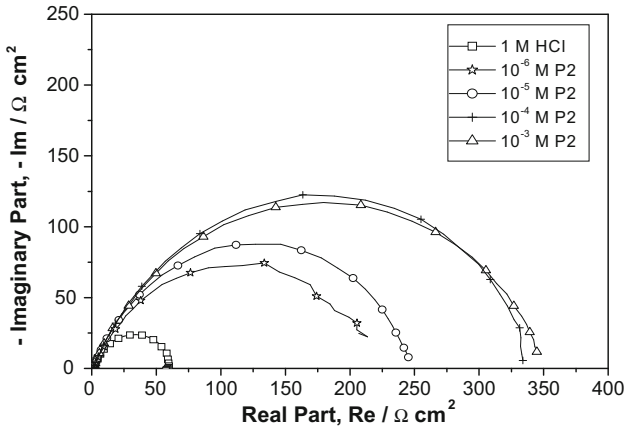

Fig. 4 Impedance diagrams under open circuit conditions for an immersion time of 30 min; C38 steel in 1 M HCl at different concentrations of P2

dispersion as a result of the non-homogeneity or the roughness of the solid state [18]. The equivalent circuit involves only one time constant ($R_e - (R_{ct} - C_{dl})$), fits well the experimental results. The intersection of the capacitive loop with the real axis represents the charge-transfer resistance, R_{ct} at very low frequencies and the electrolytic resistance R_e at very high frequencies which enclosed between the working electrode and the reference one.

The effect of addition of increasing concentrations of P2 is shown in Fig. 4. The electrochemical data derived from the recorded EIS are listed in Table 2. The double layer capacitance, C_{dl}, was derived from, frequency, at which the imaginary component of the impedance, −Im, was maximal using the relationship, Eq. 2:

$$f(-\mathrm{Im}_{\max}) = 1/2\,\pi\, C_{dl}\, R_t \tag{2}$$

The inhibition efficiencies of P2, at each concentration, were calculated from the double layer capacitance C_{dl}, using the following Eq. 3 [19]:

$$E_{C_{dl}}\% = \frac{C_{dl\,(free)} - C_{dl\,(inh)}}{C_{dl\,(free)}} \times 100 \tag{3}$$

Table 2 EIS data of C38 steel in 1 M HCl containing different concentrations of P2 at 293 K

Concentration of P2 (mol L^{-1})	R_t (Ω cm^2)	C_{dl} (μF cm^{-2})	$E_{C_{dl}}$ (%)
Blank	60	160	–
10^{-6}	213	53	66.8
10^{-5}	245	28	82.5
10^{-4}	333	16	90
10^{-3}	350	9	94.4

where, $C_{dl(free)}$ and $C_{dl(inh)}$ are the double layer capacitance values in absence and presence of P2, respectively. Inspection of the data of P2 in Fig. 4 and Table 2 reveals that addition of increasing concentration of P2 increases R_{ct} and decreases C_{dl}, and consequently enhances $E_{C_{dl}}$%till reaching its maximum value at 10^{-3} mol L^{-1}. Similar spectra were obtained in earlier works.

It is to be noted that the capacitive loop diameter of the Nyquist plots increases with rise of P2 concentration without affecting their characteristic features. This behaviour means that the inhibition action of P2 is due to its adsorption on the metal surface without altering the corrosion mechanism. Furthermore, the magnitude of C_{dl} decreases with increasing P2 concentrations. This situation can be interpreted as a result of increase in the surface coverage by P2, which led to an increase in the inhibiting efficiency (Table 2). The thickness of the protective layer, δ, is related to C_{dl} by the following Eq. 4:

$$\delta = \frac{\varepsilon\,\varepsilon_0}{C_{dl}} S \tag{4}$$

where, ε_0, ε, and S stand, respectively, for the vacuum dielectric constant ($\varepsilon_0 = 8.854 \times 10^{-14}$ F cm^{-1}), the relative dielectric constant, and the surface area. This decrease in C_{dl}, which can result from a decrease in local dielectric constant and/or an increase in the thickness of the electrical double layer, suggested that P2 function by adsorption on the C38 steel at the metal/solution interface.

Table 3 Corrosion rate of steel and inhibition efficiency at different concentrations of bipyrazolic derivatives for the corrosion of steel in 1 mol L^{-1} HCl obtained from weight loss measurements at 308 K after 24 h of immersion

Inhibitors	Concentration (mol L^{-1})	W_{corr} (mg cm^{-2} h^{-1})	E_w (%)	Surface coverage, θ
1 mol L^{-1} HCl	0	1.76	–	–
P1	10^{-6}	1.12	36.4	0.364
	10^{-5}	0.42	76.2	0.762
	5×10^{-5}	0.19	89.3	0.893
	10^{-4}	0.17	90.4	0.904
	5×10^{-4}	0.13	92.7	0.927
	10^{-3}	0.09	94.9	0.949
P2	10^{-6}	0.8	54.6	0.546
	10^{-5}	0.34	80.7	0.807
	5×10^{-5}	0.13	92.6	0.926
	10^{-4}	0.093	94.8	0.948
	5×10^{-4}	0.06	96.6	0.966
	10^{-3}	0.044	97.5	0.975

Table 4 Effect of temperature on the corrosion rate of C38 steel, using the gravimetric method, in 1 mol L^{-1} HCl (W_0) without and with P1 (W_1) and P2 (W_2) at 10^{-3} mol L^{-1} and the corresponding corrosion inhibition efficiencies for P1 and P2, respectively

Temperature (K)	1 mol L^{-1} HCl	P1		P2	
	W_0 (mg cm^{-2} h^{-1})	W_1 (mg cm^{-2} h^{-1})	E_1 (%)	W_2 (mg cm^{-2} h^{-1})	E_2 (%)
313	2.12	0.12	94.3	0.073	96.5
323	3.52	0.29	91.8	0.19	94.6
333	6.92	0.96	86.1	0.36	94.8
343	13.38	2.91	75.9	1.27	90.5
353	22.95	7.1	69.1	1.99	91.4

3.3 Weight loss measurements

The values of inhibition efficiency and corrosion rate obtained from weight loss method in the absence and presence of various concentrations of P1 and P2 are given in Table 3.

From these data, it is evident that for the studied inhibitors, the corrosion rate W_{corr} of C38 steel decreases with increase of concentration. Moreover, the protection efficiency increases with increasing the concentration of both bipyrazolic derivatives.

Inhibition efficiencies (E_w%) were calculated according to the Eq. 5:

$$E_W\% = \frac{W_{corr} - W_{corr/inh}}{W_{corr}} \times 100 \quad (5)$$

where, W_{corr} and $W_{corr/inh}$ are the corrosion rate of steel without and with inhibitors, respectively.

Maximum E_W% for each compound was achieved at 10^{-3} mol L^{-1} and any further increase in concentration did not cause appreciable change in the performance of inhibitors.

The variation in inhibiting efficiency mainly depends on the type and the nature of the substitution in the inhibitor molecule. The ability of the molecule to adsorb on the C38 steel surface was dependent on the presence of hydroxyl group –OH on P2 which arise an enhancement in the inhibiting efficiency. The same effect has been observed by Tebbji et al. for the study of two organic compounds pyridin–pyrazol type [20].

The results obtained from the weight loss measurements are in agreement with those obtained from linear polarization and EIS methods.

4 Effect of temperature

The temperature can modify the interaction between the C38 steel electrode and the acidic medium in the absence and the presence of inhibitors. Weight loss measurements for C38 steel in 1 mol L^{-1} HCl without and with 10^{-3} mol L^{-1} of P1 and P2, in the temperature range 313–353 K, are shown in Table 4.

The corrosion rates increase with rise of temperature both in uninhibited and inhibited solutions. Moreover, the C38 steel corrosion increased more rapidly with temperature in the presence of P1 than with P2. Therefore the values of inhibiting efficiency of P2 decrease slightly with

temperature increase but the protective properties are very good even at 353 K (91.4%). Whereas, the inhibiting efficiency of P1 with less protective properties decreases markedly with temperature increases—its value reaches 69.1% at 353 K. These results confirm that P2 acts as the best inhibitor in the range of temperature studied. The P2 inhibitor efficiency was then nearly temperature-independent.

The corrosion reaction can be regarded as an Arrhenius-type process, Eq. (6) [21, 22]:

$$W_{corr} = A\, e^{-\frac{E_a}{RT}} \tag{6}$$

where W_{corr} is the corrosion rate, A is the Arrhenius pre-exponential constant and E_a is the activation corrosion energy for the corrosion process:Activation parameters for the corrosion process were calculated using the alternative form of the Arrhenius equation called transition state, Eq. 7 [23]:

$$W_{corr} = \frac{k_B T}{h} \exp\left(\frac{\Delta S*}{R}\right) \exp\left(-\frac{\Delta H*}{RT}\right) \tag{7}$$

where k_B is the Boltzmann's constant ($k_B = 1.38066\ 10^{-23}$ J K^{-1}), h is the Planck's constant ($h = 6.6252\ 10^{-34}$ J s) and ΔH* and ΔS* are the enthalpy and the entropy of corrosion process activation, respectively.

The apparent activation energies E_a and pre-exponential factors A at 10^{-3} mol L^{-1} of bipyrazolic derivatives are calculated by linear regression between ln (W_{corr}) and 1/T (Fig. 5) The results are shown in Table 5.

All the linear regression coefficients R^2 are close to 1, indicating that the steel corrosion in inhibited and uninhibited media can be elucidated using the kinetic model. The pre-exponential factor A and E_a show the same trend. Table 4 also shows that the values of E_a, determined in the presence of P1 and P2, are lower than in free solution (blank). The E_a value corresponds to that of hydrogen ions activation and in fact can be considered as a verification of the corrosion process [24].

The temperature dependence of the inhibiting effect and the comparison of the values of the apparent activation energy of the corrosion process in absence and presence of inhibitors can provide further evidence [25, 26] concerning the mechanism of the inhibiting action. The decrease of the inhibitor efficiency with temperature rise, which refers to a higher value of E_a, when compared to that in an acid with no inhibitor, is interpreted as an indication for an electrostatic character of the inhibitor's adsorption. The lower value of E_a in an inhibited solution when compared to that for an uninhibited one shows that strong chemisorption bond between the inhibitor and the metal is highly probable. Hence it can be suggested that P1 and P2 adsorb on the metal surface forming strong chemisorption bonds. This is in fact possible in view of the presence of unshared electron pairs in the organic compounds molecules and taking into consideration the behaviour of iron as electrons acceptor (its d-submonolayer is incomplete).

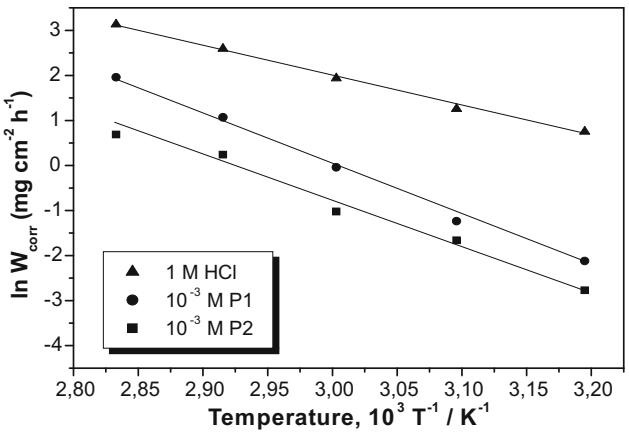

Fig. 5 Arrhenius plots of C38 steel in 1 mol L^{-1} HCl without and with P1 at 10^{-3} mol L^{-1} and P2 at 10^{-3} mol L^{-1}

Figure 6 shows the plot of ln (W_{corr}/T) against 1/T. Straight lines are obtained with a slope of (−ΔH*/R) and an intercept of (ln k_B/h + ΔS*/R), which give the values of ΔH* and ΔS*.

Positive entropy of activation is obtained in the presence of P1, while negative value is observed in the case of P2. Such variation is attributed to the phenomena of ordering and disordering of the inhibitors onto the electrode surface. The increase of ΔS* reveals that an increase in disordering takes place on going from reactants to the activated complex [27].

Inspection of the curves (Fig. 6) and the values of ΔS* and ΔH* data in Table 5 reveals that the thermodynamic parameters ΔH* of the dissolution reaction of steel in 1 mol L^{-1} HCl in the presence of P1 and P2 are higher

Table 5 Activation parameters E_a, ΔH* and ΔS* of C38 steel dissolution in 1 mol L^{-1} HCl in the absence and the presence of 10^{-3} mol L^{-1} P1 and P2

	R^2	A (mg cm^{-2} h^{-1})	E_a (kJ mol^{-1})	ΔH* (kJ mol^{-1})	ΔS* (J K^{-1} mol^{-1})
1 mol L^{-1} HCl	0.99816	1.17×10^{15}	96.1	53.2	−69.7
10^{-3} mol L^{-1} P1	0.99295	2.29×10^{12}	81.2	93.3	34.3
10^{-3} mol L^{-1} P2	0.99793	4.32×10^{9}	56.0	75.5	−26.1

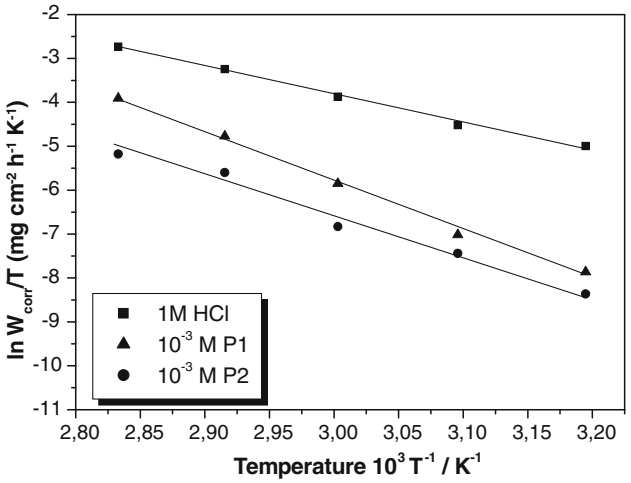

Fig. 6 Arrhenius plots of ln (W_{corr}/T) versus 1/T in 1 mol L^{-1} HCl without and with P1 at 10^{-3} mol L^{-1} and P2 at 10^{-3} mol L^{-1}

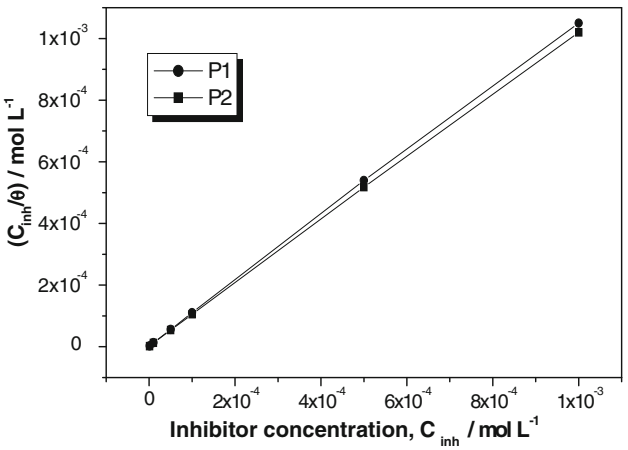

Fig. 7 Langmuir isotherm adsorption model on the steel surface of P1 and P2 in 1 M HCl

than that of in the absence of inhibitors. The positive signs of the enthalpies ΔH* reflect the endothermic nature of the steel dissolution process and it indicates that the dissolution of steel is difficult [28].

5 Adsorption isotherm

Important information about the interaction between the inhibitor and C38 steel surface can be provided by the adsorption isotherm. From the above results, it could be concluded that the surface coverage θ (E_W%/100) increases with the inhibitor concentration; this is attributed to more adsorption of inhibitor molecules onto the steel surface. As it is known, the adsorption of inhibitor is always a displacement reaction involving removal of absorbed water molecules from the metal surface, Eq. 8 [29]:

$$\text{Org (sol)} + n\text{H}_2\text{O(ads)} = \text{Org (ads)} + n\text{H}_2\text{O(sol)} \qquad (8)$$

where Org (sol) and Org (ads) are the organic molecules in the aqueous solution and adsorbed on the steel surface, respectively. H_2O (ads) is the water molecule on the steel surface and n reflects the size ratio representing the number of water molecules replaced by one unit of inhibitors.Now, assuming that the adsorption of bipyrazolic belonged to the monolayer adsorption, then the Langmuir adsorption isotherm is applied to investigate the mechanism by the Eq. 9 [30]:

$$\frac{C_{inh}}{\theta} = C_{inh} + \frac{1}{K_{ads}} \text{with } \Delta G_{ads} = -RT \ln 55.55 K_{ads} \qquad (9)$$

where K_{ads} is the adsorption coefficient and ΔG_{ads} is the free energy of adsorption values of P1 and P2.

The plot (Fig. 7) of C_{inh}/θ versus C_{inh} with slope around unity suggests that P1 and P2 adsorb on the metal surface obeying to the Langmuir's adsorption isotherm. Resulted in −41.79 kJ mol^{-1} P1 and −42.86 kJ mol^{-1} P2 (Table 6) for the experimental conditions of this paper. The low and negative value of ΔG_{ads} indicated the spontaneous adsorption of inhibitor on the C38 steel surface. This kind of isotherm, generally regarded to indicate chemisorption [31], involves the assumption of no interaction between the adsorbed species on the electrode surface [32].

Table 6 Thermodynamic parameters for the adsorption of bipyrazolic derivatives in 1 mol L^{-1} HCl on C38 steel at 308 K

	K_{ads}	Slope	ΔG_{ads} kJ mol^{-1}
P1	2.20×10^5	1.05	−41.79
P2	3.35×10^5	1.02	−42.86

6 Conclusion

Concluding the experimental part, it was clearly demonstrated that all techniques used, especially electrochemical techniques are able to characterize and follow the inhibition of corrosion process promoted by the bipyrazolic molecules. The polarization curves indicated a mixed-type suppression of both anodic and cathodic processes. For inhibitors studied; the substitution of –OH group in the compound (P1) by a group $–CH_3$ (P2); has no influence on the concentration effect; on the other hand this has a tremendous influence on the temperature effect.

The thermodynamic parameters indicated that both P1 and P2 are chemisorbed on the metal surface and their adsorption obeys to the Langmuir adsorption isotherm model.

References

1. Zerga B, Sfaira M, Rais Z, Ebn Touhami M, Taleb M, Hammouti B, Imelouane B, Elbachiri A (2009) Matér Tech 97:297
2. Chaieb E, Bouyanzer A, Hammouti B, Benkadour M (2005) Appl Surf Sci 246:199
3. Bouklah M, Hammouti B (2006) Port Electrochim Acta 24:457
4. Bouyanzer A, Majidi L, Hammouti B (2007) Phys Chem News 37:70
5. Bouyanzer A, Hammouti B (2004) Pigment Resin Technol 33:287
6. Benabdellah M, Benkaddour M, Hammouti B, Bendahou M, Aouniti A (2006) Appl Surf Sci 252:6212
7. Aloui S, Forsal I, Sfaira M, Ebn Touhami M, Taleb M, Filali Baba M, Daoudi M (2009) Portugaliae Electrochim Acta 27:599
8. Kustu C, Emregul KC, Atakol O (2007) Corros Sci 49:2800
9. Zhang QB, Hua YX (2009) Electrochim Acta 54:1881
10. Radi S, Attayibat A, Ramdani A, Lekchiri Y, Hacht B, Morcellet M, Bacquet M, Willai S (2007) Bull Korean Chem Soc 28:474
11. Touhami F, Aouniti A, Abed Y, Hammouti B, Kertit S, Ramdani A, Elkacemi K (2000) Corros Sci 42:929
12. Elayyachy M, Elkodadi M, Aouniti A, Ramdani A, Hammouti B, Malek F, Elidrissi A (2005) Mater Chem Phys 93:281
13. Bentiss F, Bouanis AM, Mernari B, Traisnel M, Vezin H, Lagreneé M (2007) Appl Surf Sci 253:3696
14. Bentiss F, Gassama F, Barbry D, Gengembre L, Vezin H, Lagrenée M, Traisnel M (2006) Appl Surf Sci 252:2684
15. Cole KS, Cole RH (1941) J Chem Phys 9:341
16. Duval S, Keddam M, Sfaira M, Srhiri A, Takenouti H (2002) J Electrochem Soc 149:B520
17. Davidson DW, Cole RH (1951) J Chem Phys 19:1484
18. Stoynov ZB, Grafov BM, Savova-Stoynova B, Elkin VV (1991) Electrochemical impedance. Nauka, Moscow
19. Lagrenée M, Mernari B, Bouanis M, Traisnel M, Bentiss F (2004) Corros Sci 44:573
20. Tebbji K, Oudda H, Hammouti B, Benkaddour M, El Kodadi M, Ramdani A (2005) Colloids Surf A Physicochem Eng Asp 259:143
21. Popova A (2007) Corros Sci 49:2144
22. Stoyanova AE, Sokolova EI, Raicheva SN (1997) Corros Sci 39:1595
23. Bockris JO'M, Reddy AKN (1977) Modern electrochemistry, vol 2. Plenum Press, New York, p 1267
24. Zhuk NP (1976) Course on corrosion and metal protection. Metallurgy, Moscow
25. Szauer T, Brandt A (1981) Electrochim Acta 26:1209
26. Ivanov ES (1986) Inhibitors for metal corrosion in acid media. Metallurgy, Moscow
27. Khamis E, Hosney A, El-Khodary S (1995) Afinidad 52:209
28. Guan NM, Xueming L, Fei L (2004) Mater Chem Phys 86:59
29. Ozcan M, Dehri I, Erbil M (2004) Appl Surf Sci 236:155
30. Langmuir I (1947) J Am Chem Soc 39:1848
31. El-Khair A, Khalifa OR, Abdelhamid IA (1987) Corros Prevent Contr 34:1952
32. Bard AJ, Faulkner LR (1980) Electrochemical methods. Wiley, New York, p 517